

Research Article

Study about Doping Ion La^{3+} onto Surface of Pyrolusite Ore for Removing Simultaneously Both Fluoride and Phosphate from Wastewater

Nguyen Thi Hue and Nguyen Hoang Tung

Institute of Environmental Technology, Vietnam Academy of Science and Technology, 18 Hoang Quoc Viet Road, Cau Giay District, Hanoi, Vietnam

Correspondence should be addressed to Nguyen Thi Hue; nthue2003@gmail.com

Received 3 July 2016; Accepted 17 October 2016; Published 3 January 2017

Academic Editor: Wenshan Guo

Copyright © 2017 N. Thi Hue and N. Hoang Tung. This is an open access article distributed under the Creative Commons Attribution License, which permits unrestricted use, distribution, and reproduction in any medium, provided the original work is properly cited.

Lanthanum has been doped onto the surface of the natural Pyrolusite for simultaneous removal of phosphate and fluoride in aqueous solution. The adsorbent characterization of the materials was observed by the SEM, BET, and XRD techniques. The dynamics and isotherms models of fluoride and phosphate adsorption, with respect to pH, pH_{PZC} , adsorbent dose, and effect of coexisting ions, were studied. The results showed that lanthanum doped Pyrolusite ore (LDPO) relatively highly adsorbed amount of phosphate and fluoride from aqueous solution. Phosphate and fluoride removal efficiencies of LDPO are approximately 97% and 95%, respectively. Pseudo-first order for kinetic studies of phosphate and fluoride removal of the LDPO was observed with high correlations for fluoride but weak correlations for phosphate. However, pseudo-second order for kinetic studies was high correlation for both phosphate and fluoride. The phosphate and fluoride adsorption capacities of the LDPO significantly decreased with the existence of coions (sulfate, chloride, and nitrate) in the aqueous solution.

1. Introduction

Extensive research has been performed to eliminate phosphate or fluoride from aqueous solution due to their hazardous effect caused to the human health. Several methods such as adsorption [1–5], precipitation [6–9], ion exchange [10, 11], reverse osmosis [12, 13], nanofiltration membrane [14, 15], Donnan dialysis [16, 17], and electrodialysis [18, 19] techniques have been used for removal of either phosphate or fluoride. Amongst the mentioned methods, adsorption is a conventional technique which is widely used for removing phosphate and fluoride of water because it is economical, practicable, environmentally safe, and efficient. Various aluminum salts are combined along with inorganic or organic compounds to phosphate- or fluoride-contaminated water to form flocs [20, 21]. The flocs in turn remove either phosphate or fluoride by adsorption or by coprecipitation. Use of calcite to remove the above-mentioned compounds from aqueous solution by precipitation method has been

investigated by many authors [8, 9, 22, 23]. Reardon and Wang [8] studied fluoride removal using a lime stone reactor where the dissolution of calcite occurred to form CaF_2 precipitate. Otherwise, various adsorbents, activated alumina [24–26], activated carbon [27, 28], low cost adsorbents [5, 29–31], rare earth oxides [32, 33], and natural products [29, 30, 34, 35] like tree bark, groundnut husk, sawdust, rice husk, and so forth, have widely been used for removal of either phosphate or fluoride.

Lanthanum, a transition metal, is applied in many studies due to environmentally friendly characteristic and being relatively abundant in the Earth's crust [34, 36]. This element is known to have a high affinity for phosphate and the lanthanum-phosphate complex was even formed in low concentrations of phosphate [37, 38]. As a result, considerable attention has been focused on the use of lanthanum-containing materials for the removal of phosphate in recent years [34, 37, 38]. Likewise several adsorbents for fluoride also are lanthanum enriched materials [39–41]. On the other

hand, iron is studied for removal of phosphate in aqueous solution [1, 42]. Therefore, in this study, natural Pyrolusite, a kind of popular ores in Northern Vietnam with low cost and high amount of iron (III) ion, was doped La^{3+} for removing phosphate and fluoride and also its adsorption abilities were estimated. The La^{3+} -doped Pyrolusite ore (LDPO) was expected to develop a new material for simultaneous removal of both phosphate and fluoride in aqueous solution.

2. Materials and Methods

2.1. Materials. The Pyrolusite ore from Cao Bang province, Northern Vietnam, contains approximate 4.7% of iron calculated from amount of Fe_2O_3 .

All chemical reagents used in the experiments were of analytical grade purchased from Merck (Germany), mainly including lanthanum nitrate ($\text{La}(\text{NO}_3)_3 \cdot 6\text{H}_2\text{O}$), sodium hydroxide (NaOH), anhydrous sodium phosphate (Na_3PO_4), sodium fluoride (NaF), and nitric acid (HNO_3).

Deionized water from Milli-Q water purification system was used throughout all experiment processes of this study.

2.2. Preparation of La^{3+} -Doped Pyrolusite Ore (LDPO). The LDPO was synthesized by traditional coprecipitation method of lanthanum and iron in solution. The natural Pyrolusite ore and $\text{La}(\text{NO}_3)_3 \cdot 6\text{H}_2\text{O}$ were simultaneously stirred in HNO_3 solution to dissolve lanthanum and also part of the iron of Pyrolusite into the solution. The above dissolved elements were then coprecipitated in the form of its hydroxides or oxides by the $\text{NaOH} + \text{H}_2\text{O}_2$ mixed solution and they are set onto the surface of the material. By this way, the new fresh layer of Pyrolusite was created. The material was filtered, dried at the temperature lower than 70°C and washed out of NaCl , and then dried again in the same above-mentioned condition.

In order to choose the most optimal LDPO for removal of phosphate and fluoride, lanthanum was added with various molar ratios between La^{3+} and the iron (Fe^{3+}), which was dissolved from the Pyrolusite into the solution. LDPO-0 was without La^{3+} doped onto surface of the Pyrolusite; LDPO 1:3, 1:2, 1:1, 2:1, and 3:1 were ratios of molar between La^{3+} and Fe^{3+} covered on the surface of the Pyrolusite, respectively.

2.3. Estimation of Amount of Phosphate and Fluoride Ions Adsorbed by LDPO. The adsorbent was added to a solution containing phosphate (30 mg/L) and fluoride (10 mg/L). After that, the solution was stirred for 2 hrs at 25°C and pH of 6. The sample was then filtrated through a Whatman $0.45 \mu\text{m}$ membrane filter, and the filtrate concentration of phosphate and fluoride was analyzed by the absorption spectrophotometer (880 nm for phosphate and 570 nm for fluoride, UV-Vis 2450, Shimadzu, Japan). The analytical procedure of the concentration of phosphate and fluoride was performed according to Standard Methods for the Examination of Water and Waste Water Fluoride: SMEWW 4500-F⁻. B&D: 2012. Phosphate: SMEWW 4500-P.E: 2012. The amount of

phosphate and fluoride ions adsorbed onto the adsorbent at equilibrium was calculated by the following equation:

$$q_e = \frac{(C_0 - C_e)V}{W}, \quad (1)$$

where q_e is the amount adsorbed at equilibrium (mg/g); C_0 is the initial concentration (mg/L); C_e is the equilibrium concentration (mg/L); V is the volume of the solution; and W is the weight of the adsorbent (g).

2.4. Characterizations of LDPO. This study used 3 methods for estimating characterizations of the adsorbents. The morphologies were determined by scanning electron microscopy (JEOL JSM-7600F, USA). Energy-dispersive X-ray (EDX) spectroscopy for detecting the elements was performed on Oxford Instruments 50 mm^2 X-Max (UK). The surface area was measured by the BET surface area analyzer (Micromeritics 3 Flex, USA).

2.5. Adsorption Dynamic and Isotherm Studies of LDPO. In order to study adsorption dynamics, phosphate solutions of 30, 50, and 100 mg/L and fluoride solutions of 10, 15, and 20 mg/L concentrations were investigated at the initial pH value of 6.0. 100 mL of both phosphate and fluoride containing solution was stirred with definite amount of adsorbent for different time durations ranging from 60 to 300 min at pH of 6.0. After the contact time, the adsorbent was separated from the solution by filtration and the remaining concentration of phosphate and fluoride in the solution was determined.

Phosphate and fluoride adsorption isotherms on LDPO at the pH value of 6.0 were studied at different temperatures (20 , 30 , and 40°C) by varying the initial concentrations of both phosphate and fluoride. In each experiment, 0.1 g of the adsorbent was transferred into the 250 mL conical flask and 100 mL of solution containing different concentrations of phosphate and fluoride was then added to the flask. After the reaction period, all samples were filtered by a Whatman $0.45 \mu\text{m}$ membrane filter and concentrations of phosphate and fluoride were analyzed. The amounts of adsorbed phosphate or fluoride were calculated by the difference in the initial and residual amounts of phosphate or fluoride in solution divided by the weight of the adsorbent.

3. Result and Discussions

3.1. Phosphate and Fluoride Removal Potential of La^{3+} -Doped Pyrolusite Ores (LDPOs). Possibility of phosphate and fluoride removal by LDPOs was investigated in this study. Figure S1A (in Supplementary Material available online at <https://doi.org/10.1155/2017/4893835>) presented the results for simultaneous removal of phosphate and fluoride from aqueous solutions by different LDPOs (LDPO 1:3, 1:2, 1:1, 2:1, and 3:1) including natural Pyrolusite ore (NPO). It is observed that LDPO 1:1 displays highest (97.1%) phosphate and (95.3%) fluoride removal from water while the remaining LDPOs expressed removal result of phosphate (55.4%–89.6%) and fluoride (43.2%–88.9%) at 10 mg/L initial fluoride concentration level and 30 mg/L initial phosphate concentration

level. NPO removes approximately 22.2% of phosphate and 10.1% of fluoride, indicating significant changes in properties of LDPOs with respect to NPO.

In order to understand the mechanism of phosphate and fluoride removal from aqueous solutions by LDPOs and the role of hydroxide ions, resultant pH values of treated samples were measured. The treated water pH changed in range from 6.9 to 8.6 (Figure S1B). The results indicated that LDPO 1:1, which removes both phosphate and fluoride to the highest degree, gives pH of treated water at the neutral level (7.5). Therefore, LDPO 1:1 did not significantly release hydroxide ion into water in adsorption process of phosphate and fluoride.

The results show that LDPO 1:1, denoted as LDPO-G, has good potential of phosphate and fluoride removal from aqueous solution. Hence, characterization of LDPO-G was studied to understand the possible adsorption mechanisms and also useful properties.

3.2. Characterization of LDPO-G. SEM analysis was performed to understand the morphology of natural Pyrolusite ore and LDPO-G and given in Figures 1(a) and 1(b), respectively. The surfaces of natural Pyrolusite ore exhibit rough surface morphology. Natural Pyrolusite has bulky structure with no porosity and poor surface area. SEM of LDPO-G gives the changes in morphology of the Pyrolusite after lanthanum was doped and was shown in Figure 1(b). From SEM images oval shaped particles of lanthanum hydroxide dispersed on the surface of LDPO-G are clearly seen.

The surface area of the natural Pyrolusite ore was measured using the BET surface area analyzer (Micromeritics 3 Flex, USA) and was found to be $25.92 \text{ m}^2/\text{g}$. The cumulative pore volume of the adsorbent was $0.05 \text{ cm}^3/\text{g}$. Values of these parameters indicate the natural Pyrolusite ore to be a suitable adsorbent. Lanthanum modification has changed the surface morphology of the natural Pyrolusite and the BET surface area of LDPO-G was found to be $72.63 \text{ m}^2/\text{g}$ with a pore volume of $0.34 \text{ cm}^3/\text{g}$.

Energy-dispersive X-ray (EDX) analysis was employed to analyze the elements of LDPO-G. The EDX pattern of the LDPO-G was shown in Figure 2. A component with riches of lanthanum (19.81%), iron, and so forth was observed (Table S1). The EDX spectrum of the LDPO-G (Figure 2) shows the presence of lanthanum along with other principal elements. The result provided an evidence for the lanthanum ion successfully doped onto the surface of the LDPO-G.

3.3. pH of Point of Zero Charge (pH_{PZC}) of LDPO-G. The pH of point of zero charge (pH_{PZC}) is an important interfacial parameter used widely in characterizing the ionization behavior of a surface. The pH_{PZC} of the adsorbent was investigated according to experiments of Teng et al. and Sharma et al. [52, 53]. For its determination, 0.2 g of the adsorbent was transferred into 250 mL conical flasks containing 50 mL of 0.01 M NaCl solution after being adjusted to varied initial pH values (2.0–12.0) by 0.1 M HNO_3 . This setup was kept for 48 hrs and then a Whatman 0.45 μm membrane filter was used for separating the adsorbent in NaCl solutions

and final pH values of the solutions were measured. The initial and final pH values of the solutions were measured as $\text{pH}_{\text{initial}}$ and pH_{final} , respectively. pH_{PZC} is intersection point of lines joining pH initially and pH_{final} in " pH_{final} versus $\text{pH}_{\text{initial}}$ " graph. The pH_{PZC} refers to the bulk aqueous phase concentration (or, more precisely, activity) of potential-determining ions giving zero surface charge. The pH_{PZC} of LDPO-G was found to be approximate 6.8.

3.4. Effect of Solution pH on Phosphate and Fluoride Removal Potential of LDPO-G.

The role of pH is a major factor which controls the adsorption at the water-adsorbent interface [31]. In order to estimate the effect of pH on removal of phosphate and fluoride of LDPO-G, 0.1 g of LDPO-G was added to 500 mL of the solution containing 30 mg/L phosphate and 10 mg/L fluoride and, after that, the experiments were performed at various initial pH, ranging from 2.0 to 10.0. Figure 3 shows the adsorption of both phosphate and fluoride onto LDPO-G as functions of pH. Adsorption of phosphate onto LDPO-G increased with increasing pH and reached a maximum range from 4.9 mg/g to 5.1 mg/g at pH 3.0–6.0 (Figure 3). Similarly, the fluoride adsorption of LDPO-G gently increased with increasing pH and reached a maximum of 1.3 mg/g at pH 6.0 (Figure 3). Figure 3 indicated that maximum adsorption of LDPO-G is slight difference for pH values between phosphate (at pH 5) and fluoride (at pH 6.0). Therefore, in order to simultaneously adsorb both phosphate and fluoride, the value of 6.0 is considered to be the optimum pH of LDPO-G for further experimental studies.

3.5. Effect of Contact Time for Adsorbing Phosphate and Fluoride by LDPO-G.

In this study, the result indicated that maximum concentration of phosphate and fluoride removal was attained to be approximate 2 hrs and, thereafter, it almost remained static for LDPO-G. The period of contact time of 2 hrs for further studies was fixed. The phosphate and fluoride removal capacities at the pH value of 6.0 were 5.3 mg/L and 2.1 mg/L, respectively.

3.6. Effect of Adsorbent Dosage on Removal of Phosphate and Fluoride.

In order to find the minimum dosage of LDPO-G for maximum adsorption of phosphate and fluoride, the effects of adsorbent dosage were measured by varying the dosages of LDPO-G from 0.01 g to 0.1 g in aqueous solution containing phosphate and fluoride concentrations to be 30 mg/L and 10 mg/L, respectively. It was observed as shown in Figure 4 that the percentage adsorption increased with respect to the increased dosage and then remained constant after 0.08 g of both phosphate and fluoride. The increase in adsorption capacity with increase in dosage is apparent, because any adsorption process depends upon the number of active sites [54]. Increased adsorbent dosage implied a greater surface area and a greater number of binding sites available for the constant amounts of both phosphate and fluoride. The adsorbent dosage, therefore, was optimized to be 0.1 g for further experimental studies.

3.7. Adsorption Dynamics. To understand the adsorption dynamics of phosphate and fluoride removal, two types

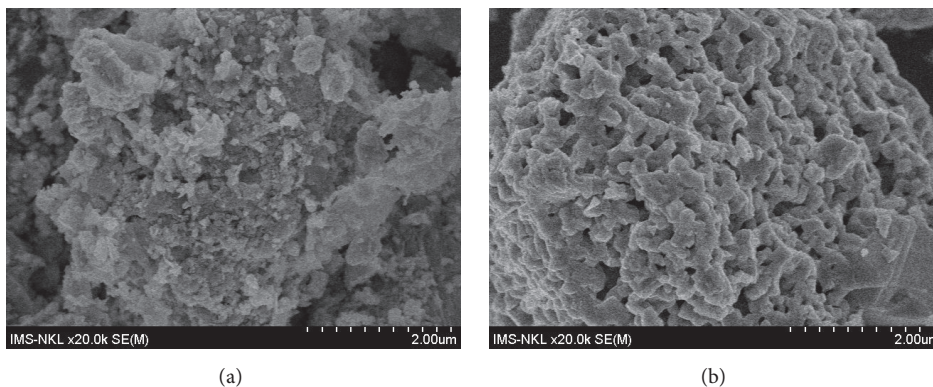


FIGURE 1: Scanning electron microscopy (SEM) image of Pyrolusite ore, (a) natural Pyrolusite ore, and (b) La^{3+} -doped Pyrolusite ore at $\text{La}^{3+}/\text{Fe}^{3+}$ molar ratio of 1:1.

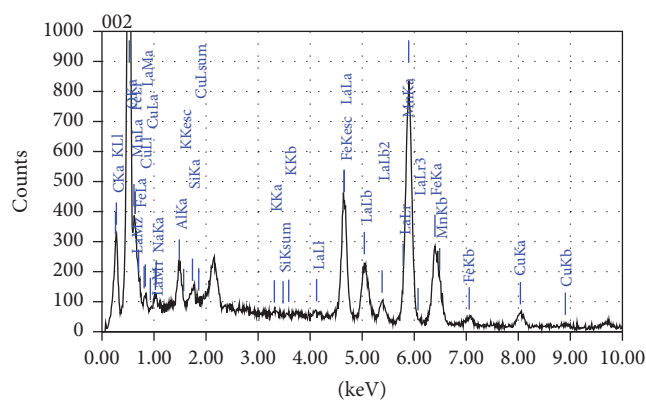


FIGURE 2: Energy-dispersive X-ray (EDX) spectrograph of LDPO-G.

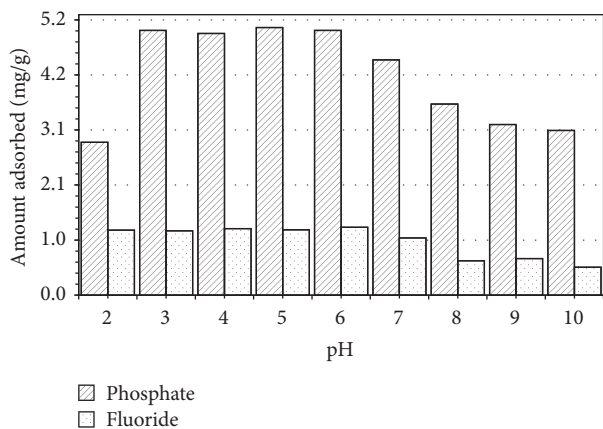


FIGURE 3: Effect of pH on adsorption of fluoride and phosphate on LDPO-G (initial concentrations of phosphate: 30 mg/L and fluoride: 10 mg/L; contact time: 2 hrs).

of models were investigated to estimate the fitness of the experimental data to pseudo-first-order and pseudo-second-order kinetic models.

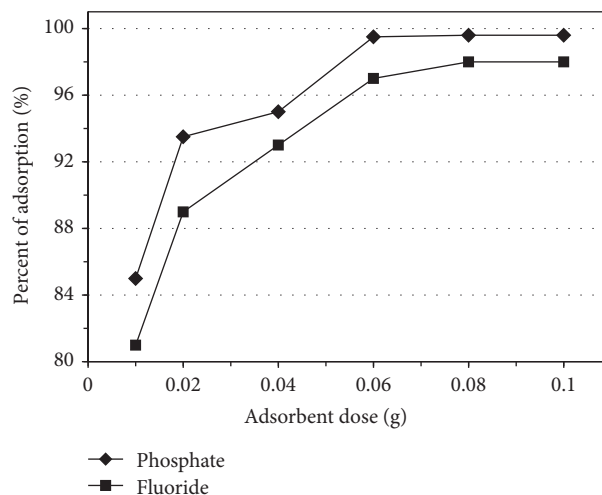


FIGURE 4: Effect of dosage on removal of fluoride and phosphate adsorption by LDPO-G.

The pseudo-first-order kinetic model [55] is represented as

$$\log(q_e - q_t) = \log q_e - \frac{k_1}{2.303} (t) \quad (2)$$

and the pseudo-second-order kinetic model [56] is as follows:

$$\frac{t}{q_t} = \frac{1}{k_2 q_e^2} + \frac{1}{q_e} t, \quad (3)$$

where q_t and q_e are the amounts (mg/g) of phosphate or fluoride adsorbed onto the surface of LDPO-G at any time t and at equilibrium; k_1 is the equilibrium rate constant of pseudo-first-order adsorption (min^{-1}); the linearity plots of $\log(q_e - q_t)$ versus t for different experimental conditions will be used to calculate the value of rate constants (k_1); k_2 is the pseudo-second-order rate constant obtained from the slope of the linear plots of t/q_t versus t for different experimental conditions.

Figures 5(a) and 5(b) show the pseudo-first-order kinetic plots of experimental data of phosphate and fluoride adsorption on LDPO-G in aqueous solutions. Table 1 presented

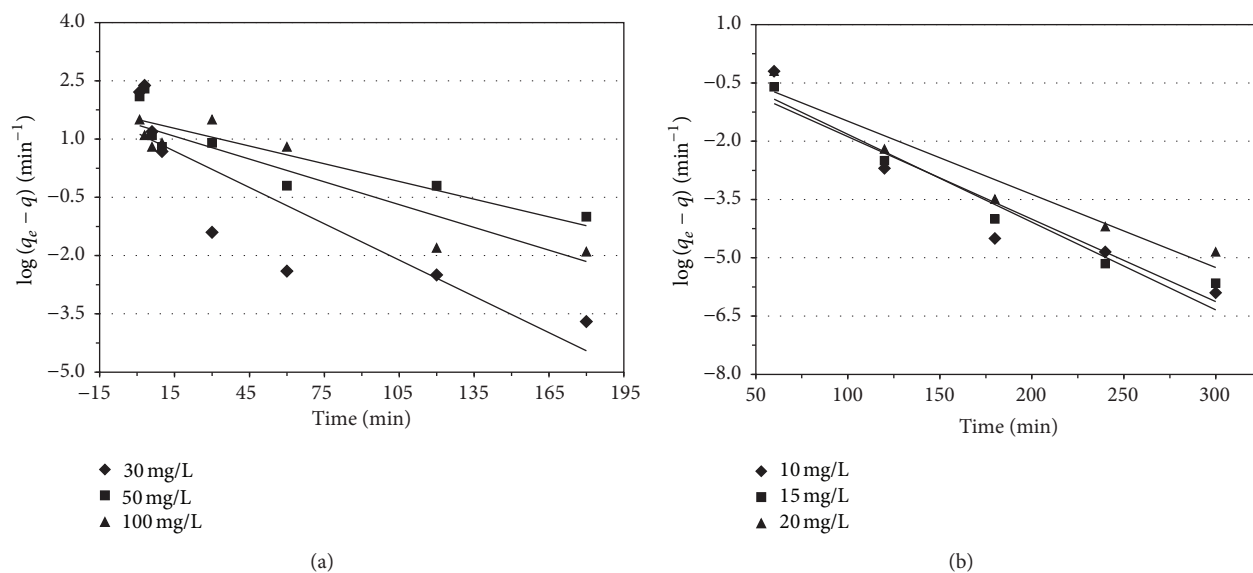


FIGURE 5: Pseudo-first-order models of LDPO-G for fluoride and phosphate removal. (a) Removal of phosphate at 30, 50, and 100 mg/L. (b) Removal of fluoride at 10, 15, and 20 mg/L.

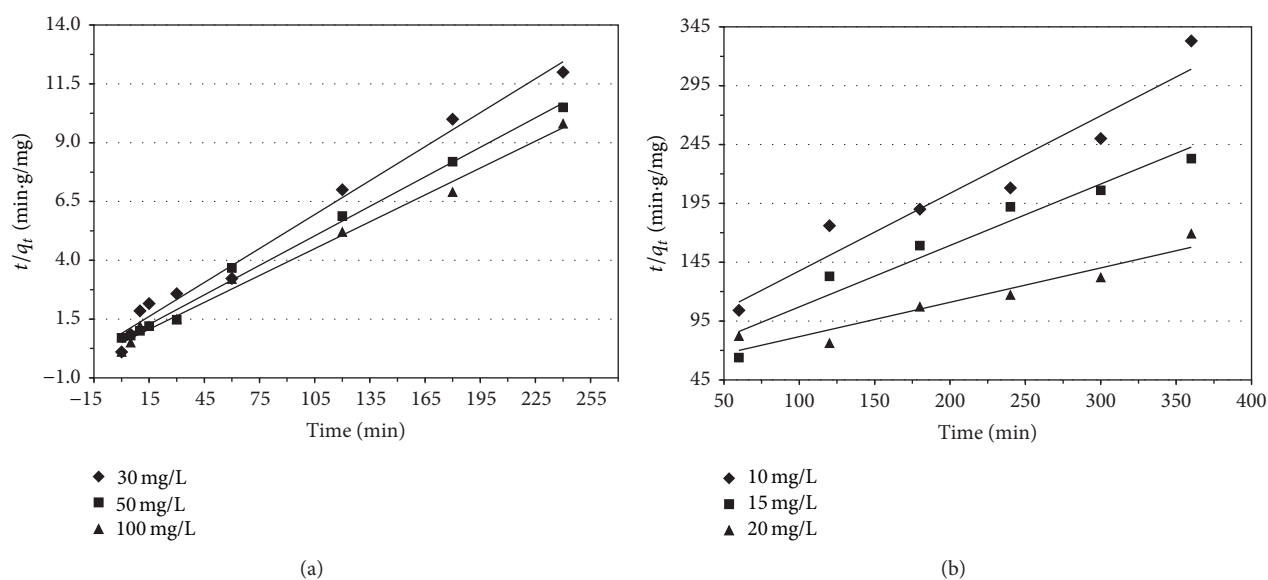


FIGURE 6: Pseudo-second-order models of LDPO-G for fluoride and phosphate removal. (a) Removal of phosphate at 30, 50, and 100 mg/L. (b) Removal of fluoride at 10, 15, and 20 mg/L.

the summary of parameters of kinetic data model fittings. For phosphate adsorption, the analysis indicates that LDPO-G did not follow first-order kinetics with significantly weak correlation (R^2) and low rate constant (k_1) at all phosphate concentrations investigated (Table 1 and Figure 5(a)). The values of R^2 were found as 0.854, 0.808, and 0.717 and also the values of k_1 were found as 0.041, 0.037, and 0.016 min⁻¹, respectively, for the selected initial concentrations of phosphate. In contrast, LDPO-G follows first-order kinetics with good correlation (R^2) for fluoride concentrations (Table 1 and Figure 5(b)). The values of R^2 were found as 0.940, 0.957, and 0.916 and also the values of k_1 were found as 0.041,

0.048, and 0.051 min⁻¹, respectively, for the selected initial concentrations of fluoride. The values of k_1 were found to be decreasing with increasing the initial concentrations of fluoride from 10 to 20 mg/L.

From Table 1, it is observed that pseudo-second-order kinetics show good correlation (R^2) for phosphate removal for all concentrations of phosphate (Table 1 and Figure 6(a)). The values of R^2 were found as 0.985, 0.994, and 0.991 and also the values of pseudo-second-order rate constant (k_2) were calculated as 0.0025, 0.0026, and 0.0029 mg/g-min at the three selected phosphate concentrations, respectively. For fluoride removal, pseudo-second-order kinetics show significantly

TABLE 1: The kinetic model parameters for the adsorption of phosphate and fluoride on LDPO.

	Conc. (mg/L)	Pseudo-first order			Pseudo-second order		
		k_1 (min^{-1})	q_e (mg/g)	R^2	k_2 (g/mg·min)	q_e (mg/g)	R^2
Phosphate	30	0.041	6.32	0.854	0.0025	20.83	0.985
	50	0.037	22.38	0.808	0.0026	24.39	0.994
	100	0.016	10.74	0.717	0.0029	26.32	0.991
Fluoride	10	0.041	2.52	0.940	0.006	1.517	0.928
	15	0.048	1.76	0.957	0.005	1.916	0.939
	20	0.051	2.72	0.916	0.002	3.436	0.913

good correlation (R^2) for concentrations of fluoride (Table 1 and Figure 6(b)). The values of R^2 were found as 0.928, 0.939, and 0.913 and also the values of k_2 were calculated as 0.006, 0.005, and 0.002 mg/g·min at the three selected fluoride concentrations, respectively. Therefore, from the good R^2 and low k_2 obtained from Figure 6, it can be concluded that the adsorption of phosphate and fluoride onto LDPO-G is governed by pseudo-second-order model.

3.8. Adsorption Isotherms. The equilibrium data have been analyzed by the linear regression of isotherm model equations, Langmuir and Freundlich.

The Langmuir isotherm model [57], which is based on adsorbent surfaces, is

$$\frac{C_e}{q_e} = \frac{1}{q_0 K_L} + \frac{C_e}{q_0} \quad (4)$$

and the Freundlich isotherm model equation [58] is as follows:

$$\log q_e = \log K_F + \frac{1}{n} \log C_e, \quad (5)$$

where q_e and C_e are the equilibrium adsorption capacity (mg/g) and the equilibrium adsorbate concentration (mg/L), respectively; q_0 is the monolayer surface coverage (mg/g) and K_L is the equilibrium adsorption constant (L/mg), and q_0 value (mg/g) was calculated from the slope of the linear plot of C_e/q_e versus C_e ; and K_F and n are empirical constants that are dependent on several environmental factors. The plot of $\log C_e$ versus $\log q_e$ of the equation mentioned above should result in a linearized plot. From the slope and the intercept of the plot, the values of n and K_F can be obtained.

The Langmuir isotherm plot in linear form for phosphate removal at three temperatures 20, 30, and 40°C has given correlation coefficients (R^2) as 0.994, 0.990, and 0.986, respectively (Figure 7(a)). The values of q_0 were obtained as 83.33, 76.92, and 66.67 mg/g (Table 2). The values of K_L were 0.026, 0.023, and 0.021 L/mg at the respective temperatures. The decreasing K_L with a rise in reaction temperatures indicated that the adsorption process of phosphate is exothermic. Similar effect of temperature on phosphate was also reported by Tian et al. [59]. On the other hand, R^2 values of the Langmuir isotherm plot for fluoride removal at 20, 30, and 40°C were 0.993, 0.995, and 0.994, respectively (Figure 7(b)). The values of q_0 were obtained as 12.82, 10.56, and 9.43 mg/g (Table 2).

The values of K_L were 0.607, 0.283, and 0.159 L/mg at the respective temperatures. The increasing K_L with increasing temperatures indicated that the interaction between fluoride and LDPO-G is the endothermic adsorption. This result is similar to reports of other researchers [60, 61].

Figure 8(a) indicated the straight line of Freundlich isotherm for phosphate adsorption on LDPO-G. The correlation coefficients (R^2) are found as 0.909, 0.932, and 0.951 at the selected temperatures 20, 30, and 40°C, respectively (Table 2). This indicates that the adsorption data of phosphate onto LDPO-G fitted well with Freundlich isotherm assumptions at these temperatures. The values of n were found as 10.8, 9.43, and 6.67 at selected temperatures (Table 2). On the other hand, the linearized plot of Freundlich isotherm for fluoride adsorption on LDPO-G was shown in Figure 8(b). R^2 values at the selected temperatures 20, 30, and 40°C were found as 0.941, 0.873, and 0.901, respectively (Table 2). This indicates that the adsorption data of fluoride on LDPO-G fitted significantly well with Freundlich isotherm assumptions at these temperatures except at 30°C. The values of n were found as 1.67, 1.79, and 1.43 at selected temperatures (Table 2). In conclusion, the adsorption processes of LDPO were monolayer for fluoride and multilayer for phosphate and the value of n in between 1 and 10 indicates useful adsorption [62]. Hence, adsorption of phosphate and fluoride on LDPO-G may be called "useful." K_F constants were found as 33.7, 18.8, and 14.1 for phosphate removal and 2.83, 5.83, and 9.53 on these respective temperatures (Table 2). The increasing values of K_F of fluoride removal with temperature indicate that adsorption is favorable at higher temperatures [53].

Many adsorbents have been tested for their either phosphate or fluoride removal potentials from aqueous solutions and some of the results were summarized in Table 3. Lanthanum was doped or modified in some material to have an adsorption capacity of phosphate from 6.70 mg/g to 108.7 mg/g [2, 44–46]. Other elements were also used for removal of phosphate in range from 2.5 mg/g to 153 mg/g [1, 3, 42, 43], while LDPO-G gives a phosphate adsorption capacity ranging from 66.7 mg/g to 76.9 mg/g with increasing temperature from 20°C to 40°C, as found in the present study. On the other hand, for position of removal of fluoride, Lanthanum was reported to be ranging from 2.74 mg/g to 23.9 mg/g [49–51] while other materials have range of fluoride removal from 0.19 mg/g to 196.1 mg/g [4, 33, 47, 48, 62]. However, in this study, LDPO-G removed a fluoride in aqueous solution ranging from 0.60 mg/g to 1.93 mg/g with increasing temperature from 20°C to 40°C.

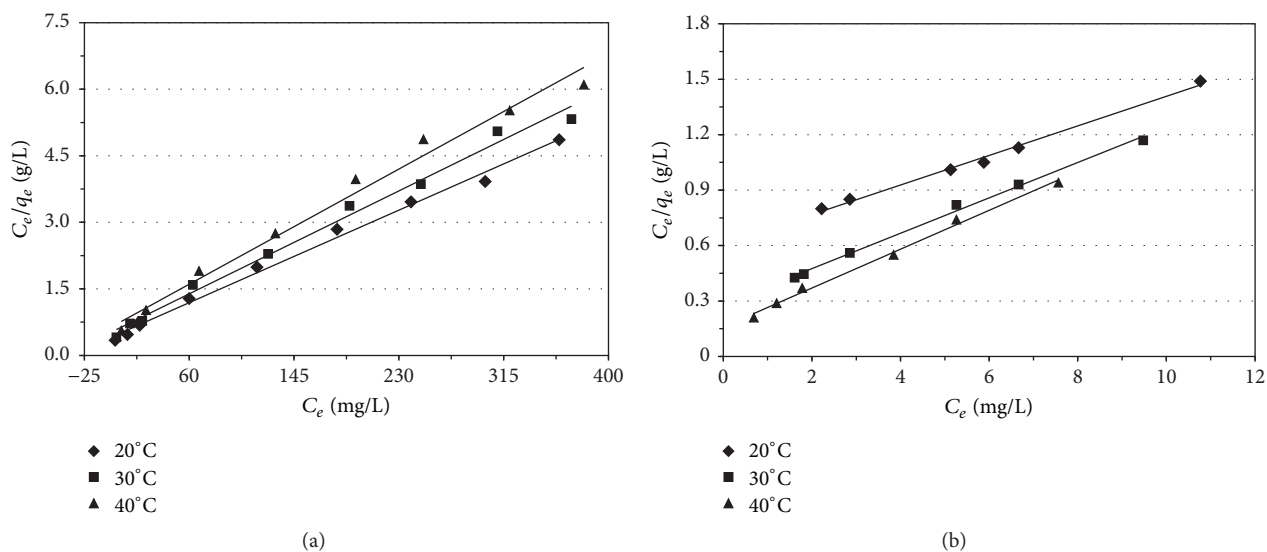


FIGURE 7: Langmuir isotherm of LDPO-G for fluoride and phosphate removal. (a) Removal of phosphate at 20, 30, and 40°C. (b) Removal of fluoride at 20, 30, and 40°C.

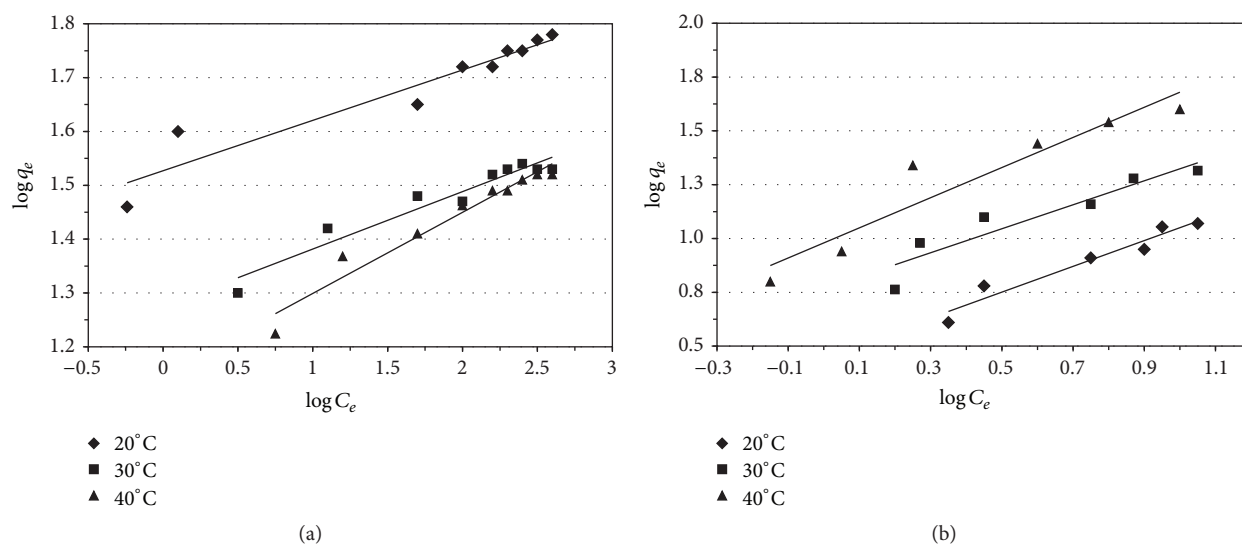


FIGURE 8: Freundlich isotherm of LDPO-G for fluoride and phosphate removal. (a) Removal of phosphate at 20, 30, and 40°C. (b) Removal of fluoride at 20, 30, and 40°C.

TABLE 2: Calculated equilibrium constants using the Langmuir and Freundlich equations for phosphate and fluoride adsorption on the LDPO.

	Temp. (°C)	Langmuir			Freundlich		
		q_0 (mg/g)	K_L (L/mg)	R^2	n	K_F (mg/g)	R^2
Phosphate	20	83.33	0.026	0.994	10.8	33.7	0.909
	30	76.92	0.023	0.990	9.43	18.8	0.932
	40	66.67	0.021	0.986	6.67	14.1	0.951
Fluoride	20	12.82	0.607	0.993	1.67	2.83	0.941
	30	10.56	0.283	0.995	1.79	5.83	0.873
	40	9.43	0.159	0.994	1.43	9.53	0.901

TABLE 3: Comparison of Langmuir and Freundlich adsorption capacities (mg/g) of various materials for removal of phosphate and fluoride.

	Adsorbents	Langmuir adsorption capacity (mg/g)	Freundlich adsorption capacity (mg/g)	References
Phosphate	Fe-Mn binary oxide	33.2	27.0	[1]
	Hydrous niobium oxide	15.0	2.9	[3]
	Calcined cobalt hydroxide	2.5–153.0	0.02–18.2	[43]
	Nano-structured Fe-Ti bimetal oxide	35.4–40.9	8.97–10.0	[42]
	La-doped vesuvianite	6.70	1.96	[44]
	La-coordinated silicates material	50.3–54.3	20.6–32.4	[2]
	La (OH) ₃ /zeolite	6.05–71.9	—	[45]
	La-modified tourmaline	67.1–108.7	7.53–17.7	[46]
	La-doped Pyrolusite ore (LDPO)	66.7–76.9	14.1–33.7	Present study
Fluoride	Mixed rare earth oxides	196.1	—	[33]
	Low cost materials	0.19–4.54	0.023–10.5	[4]
	Ti-based adsorbents	25.8–46.6	2.18–15.8	[62]
	MnO ₂ -coated tamarind fruit	0.21–0.22	—	[47]
	Mn-Ce oxide	1375	—	[48]
	La-modified activated alumina	2.74	1.26	[49]
	La-loaded bentonite/chitosan beads	3.70–8.55	0.24–0.45	[50]
	La-Al loaded scoria	23.9	1.25	[51]
	La-doped Pyrolusite ore (LDPO)	9.43–12.82	2.83–9.53	Present study

3.9. Effect of Coexisting Ions in Aqueous Solution on Removal of Phosphate and Fluoride of LDPO-G. Many coions such as sulfate, chloride, and nitrate usually exist in water and they compete with phosphate and fluoride ions during the adsorption process. Therefore, the effect of these ions in adsorption of both fluoride and phosphate by LDPO-G was carried out. The initial concentration of phosphate and fluoride was fixed 30 mg/L and 10 mg/L, respectively, while the concentrations (25–100 mg/L) of sulfate, chloride, and nitrate were varied in the adsorption studies. It can be seen that the adsorption of both fluoride and phosphate decreases with increase in coions concentrations. At 0 mg/L of the coions, phosphate and fluoride adsorbed 94.1% and 93.2%, respectively. However, the adsorption of phosphate and fluoride rapidly reduced to approximately 30% and 25% at 100 mg/L of coions.

3.10. Desorption Studies. The ultimate objective of the present work is to develop an adsorbent that can be reused thereby making it cost effective. As the adsorption becomes less at high pH (pH 10 given in Figure 3), it can be anticipated that better desorption occurs. Hence, NaOH solution was used for desorption studies of adsorbent. First the phosphate (30 mg/L) and fluoride (10 mg/L) were adsorbed onto the adsorbent (0.1 g) at pH 6.0. Then the solution was filtered and the adsorbent was transferred to 100 mL of water and the

pH was adjusted. Desorption studies were shaken in flasks at various pH (range from 3 to 10) for 2 hrs. The results of desorption studies are shown in Figure S2. In the acidic pH range, neither phosphate nor fluoride is leached. But as the pH is increased above pH 7, they start to leach back into the solution. At around pH 10, 90% of phosphate and 87% of fluoride could be desorbed in about 2 hrs.

3.11. Performance in Wastewater from the Fertilizer Factory. To evaluate the phosphate and fluoride removal performance in wastewater, LDPO was applied to treat water samples collected from the waste channel of the Superphosphate Fertilizer factory in Phu Tho province, Northern Vietnam. The phosphate and fluoride concentrations in the wastewater are detected to be 13.72 mg/L and 4.68 mg/L, respectively (data is shown in Table S2).

As shown in Figure S3, both phosphate and fluoride were effectively removed from wastewater and the removal efficiency increases with the increase of adsorbent dosage. With adsorbent dosage of 0.1 g, the phosphate and fluoride removal efficiencies of LDPO are 94% and 93%, respectively.

4. Conclusion

Transition metal La doped onto the surface of the natural Pyrolusite ore was successfully synthesized. The surface and

structure characteristics were studied by EDX, BET, and SEM analysis. In the studies about simultaneous removal of phosphate and fluoride, the La³⁺-doped Pyrolusite ore expresses rapid adsorption rate and high adsorption capacity. The capacity increases with the increase in adsorbent dosages. The optimal pH for phosphate and fluoride adsorption of the adsorbent is approximate 6.0. In addition the best condition for desorption of the adsorbent is at pH 10. Otherwise the adsorbent was preliminarily studied for treating the wastewater and the phosphate and fluoride removal performances are significantly high. Further investigations on adsorption abilities of this material in wastewater samples are needed to apply for treating phosphate- or/and fluoride-contaminated waste sources of industrial areas in Vietnam.

Competing Interests

The authors declare that they have no competing interests.

Acknowledgments

The authors would like to express special thanks to the Project of Science and Technology of “Program of Scientific Study, and Technological Application and Transfer for Developing Environmental Industry” performing “The Project of Developing Environmental Industry to 2015, and Looking Into 2025”, Ministry of Industry and Trade, Government of Vietnam, for the financial support to perform this study.

References

- [1] G. Zhang, H. Liu, R. Liu, and J. Qu, “Removal of phosphate from water by a Fe-Mn binary oxide adsorbent,” *Journal of Colloid and Interface Science*, vol. 335, no. 2, pp. 168–174, 2009.
- [2] J. Zhang, Z. Shen, W. Shan, Z. Mei, and W. Wang, “Adsorption behavior of phosphate on lanthanum(III)-coordinated diamino-functionalized 3D hybrid mesoporous silicates material,” *Journal of Hazardous Materials*, vol. 186, no. 1, pp. 76–83, 2011.
- [3] L. A. Rodrigues and M. L. C. P. da Silva, “Thermodynamic and kinetic investigations of phosphate adsorption onto hydrous niobium oxide prepared by homogeneous solution method,” *Desalination*, vol. 263, no. 1–3, pp. 29–35, 2010.
- [4] X. Fan, D. J. Parker, and M. D. Smith, “Adsorption kinetics of fluoride on low cost materials,” *Water Research*, vol. 37, no. 20, pp. 4929–4937, 2003.
- [5] M. Srimurali, A. Pragathi, and J. Karthikeyan, “A study on removal of fluorides from drinking water by adsorption onto low-cost materials,” *Environmental Pollution*, vol. 99, no. 2, pp. 285–289, 1998.
- [6] E.-H. Kim, S.-B. Yim, H.-C. Jung, and E.-J. Lee, “Hydroxyapatite crystallization from a highly concentrated phosphate solution using powdered converter slag as a seed material,” *Journal of Hazardous Materials*, vol. 136, no. 3, pp. 690–697, 2006.
- [7] Y. Wang, T. Han, Z. Xu, G. Bao, and T. Zhu, “Optimization of phosphorus removal from secondary effluent using simplex method in Tianjin, China,” *Journal of Hazardous Materials*, vol. 121, no. 1–3, pp. 183–186, 2005.
- [8] E. J. Reardon and Y. Wang, “A limestone reactor for fluoride removal from wastewaters,” *Environmental Science & Technology*, vol. 34, no. 15, pp. 3247–3253, 2000.
- [9] B. D. Turner, P. Binning, and S. L. S. Stipp, “Fluoride removal by calcite: evidence for fluorite precipitation and surface adsorption,” *Environmental Science and Technology*, vol. 39, no. 24, pp. 9561–9568, 2005.
- [10] B. D. Martin, S. A. Parsons, and B. Jefferson, “Removal and recovery of phosphate from municipal wastewaters using a polymeric anion exchanger bound with hydrated ferric oxide nanoparticles,” *Water Science and Technology*, vol. 60, no. 10, pp. 2637–2645, 2016.
- [11] M. J. Haron, W. M. Z. Wan Yunus, S. A. Wasay, A. Uchiumi, and S. Tokunaga, “Sorption of fluoride ions from aqueous solutions by a yttrium-loaded poly(hydroxamic acid) resin,” *International Journal of Environmental Studies*, vol. 48, no. 3–4, pp. 245–255, 1995.
- [12] E. M. Van Voorthuizen, A. Zwijnenburg, and M. Wessling, “Nutrient removal by NF and RO membranes in a decentralized sanitation system,” *Water Research*, vol. 39, no. 15, pp. 3657–3667, 2005.
- [13] S. V. Joshi, S. H. Mehta, A. P. Rao, and A. V. Rao, “Estimation of sodium fluoride using HPLC in reverse osmosis experiments,” *Water Treatment*, vol. 7, no. 2, pp. 207–211, 1992.
- [14] C. P. Leo, W. K. Chai, A. W. Mohammad, Y. Qi, A. F. A. Hoedley, and S. P. Chai, “Phosphorus removal using nanofiltration membranes,” *Water Science and Technology*, vol. 64, no. 1, pp. 199–205, 2011.
- [15] R. Simons, “Trace element removal from ash dam waters by nanofiltration and diffusion dialysis,” *Desalination*, vol. 89, no. 3, pp. 325–341, 1993.
- [16] S.-Y. Chen, Z. Shi, Y. Song, X.-R. Li, and Y.-L. Hu, “Phosphate removal from aqueous solution by Donnan dialysis with anion-exchange membrane,” *Journal of Central South University*, vol. 21, no. 5, pp. 1968–1973, 2014.
- [17] Z. Amor, B. Bariou, N. Mameri, M. Taky, S. Nicolas, and A. Elmidaoui, “Fluoride removal from brackish water by electro-dialysis,” *Desalination*, vol. 133, no. 3, pp. 215–223, 2001.
- [18] Y. Zhang, E. Desmidt, A. Van Looveren, L. Pinoy, B. Meeschaert, and B. Van Der Bruggen, “Phosphate separation and recovery from wastewater by novel electro-dialysis,” *Environmental Science and Technology*, vol. 47, no. 11, pp. 5888–5895, 2013.
- [19] T. Ruiz, F. Persin, M. Hichour, and J. Sandeaux, “Modelisation of fluoride removal in Donnan dialysis,” *Journal of Membrane Science*, vol. 212, no. 1–2, pp. 113–121, 2003.
- [20] K. R. Bulusu, B. B. Sundaresan, B. N. Pathak, and W. G. Nawlakhe, “Fluorides in water, defluoridation methods and their limitations,” *Journal of the Institution of Engineers*, vol. 60, pp. 1–25, 1979.
- [21] J.-P. Boisvert, T. C. To, A. Berrak, and C. Jolicoeur, “Phosphate adsorption in flocculation processes of aluminium sulphate and poly-aluminium-silicate-sulphate,” *Water Research*, vol. 31, no. 8, pp. 1939–1946, 1997.
- [22] J. Kleiner, “Cocprecipitation of phosphate with calcite in lake water: a laboratory experiment modelling phosphorus removal with calcite in Lake Constance,” *Water Research*, vol. 22, no. 10, pp. 1259–1265, 1988.
- [23] M. Yang, T. Hashimoto, N. Hoshi, and H. Myoga, “Fluoride removal in a fixed bed packed with granular calcite,” *Water Research*, vol. 33, no. 16, pp. 3395–3402, 1999.

- [24] O. J. Hao and C. P. Huang, "Adsorption characteristics of fluoride onto hydrous alumina," *Journal of Environmental Engineering*, vol. 112, no. 6, pp. 1054–1069, 1986.
- [25] Y. Ku and H.-M. Chiou, "The adsorption of fluoride ion from aqueous solution by activated alumina," *Water, Air, and Soil Pollution*, vol. 133, no. 1-4, pp. 349–360, 2002.
- [26] J. Xie, Y. Lin, C. Li, D. Wu, and H. Kong, "Removal and recovery of phosphate from water by activated aluminum oxide and lanthanum oxide," *Powder Technology*, vol. 269, pp. 351–357, 2014.
- [27] R. Leyva Ramos, J. Ovalle-Turrubiarres, and M. A. Sanchez-Castillo, "Adsorption of fluoride from aqueous solution on aluminum-impregnated carbon," *Carbon*, vol. 37, no. 4, pp. 609–617, 1999.
- [28] L. Zhang, L. Wan, N. Chang et al., "Removal of phosphate from water by activated carbon fiber loaded with lanthanum oxide," *Journal of Hazardous Materials*, vol. 190, no. 1–3, pp. 848–855, 2011.
- [29] S. S. Tripathy, S. B. Srivastava, J. L. Bersillon, and K. Gopal, "Removal of fluoride from drinking water by using low cost adsorbents," in *Proceedings of the 9th FECS Conference and 2nd SFC Meeting on Chemistry and the Environment*, p. 352, Bordeaux, France, 2004.
- [30] K. Gopal, S. B. Srivastava, S. Shukla, and J. L. Bersillon, "Contaminants in drinking water and its mitigation using suitable adsorbents: an overview," *Journal of Environmental Biology*, vol. 25, no. 4, pp. 469–475, 2004.
- [31] S. S. Tripathy, J.-L. Bersillon, and K. Gopal, "Removal of fluoride from drinking water by adsorption onto alum-impregnated activated alumina," *Separation and Purification Technology*, vol. 50, no. 3, pp. 310–317, 2006.
- [32] R. H. Byrne, X. Liu, and J. Schijf, "The influence of phosphate coprecipitation on rare earth distributions in natural waters," *Geochimica et Cosmochimica Acta*, vol. 60, no. 17, pp. 3341–3346, 1996.
- [33] A. M. Raichur and M. J. Basu, "Adsorption of fluoride onto mixed rare earth oxides," *Separation and Purification Technology*, vol. 24, no. 1-2, pp. 121–127, 2001.
- [34] E. W. Shin, K. G. Karthikeyan, and M. A. Tshabalala, "Orthophosphate sorption onto lanthanum-treated lignocellulosic sorbents," *Environmental Science & Technology*, vol. 39, no. 16, pp. 6273–6279, 2005.
- [35] T. S. Anirudhan, B. F. Noeline, and D. M. Manohar, "Phosphate removal from wastewaters using a weak anion exchanger prepared from a lignocellulosic residue," *Environmental Science & Technology*, vol. 40, no. 8, pp. 2740–2745, 2006.
- [36] S. Tokunaga, S. A. Wasay, and S.-W. Park, "Removal of arsenic(V) ion from aqueous solutions by lanthanum compounds," *Water Science and Technology*, vol. 35, no. 7, pp. 71–78, 1997.
- [37] P. B. Melnyk, J. D. Norman, and M. Wasserlauf, "Lanthanum precipitation. Alternative method for removing phosphates from waste water," in *Proceedings of the 11th International Rare Earths Conference*, pp. 4–13, 1974.
- [38] H. L. Recht, M. Ghassemi, and E. V. Kleber, "Precipitation of phosphates from water and waste water using lanthanum salts," in *Proceedings of the 5th International Water Pollution Research*, San Francisco, Calif, USA, 1970.
- [39] M. S. Onyango, Y. Kojima, A. Kumar, D. Kuchar, M. Kubota, and H. Matsuda, "Uptake of fluoride by Al^{3+} pretreated low-silica synthetic zeolites: adsorption equilibrium and rate studies," *Separation Science and Technology*, vol. 41, no. 4, pp. 683–704, 2006.
- [40] S. Samatya, Ü. Yüksel, M. Yüksel, and N. Kabay, "Removal of fluoride from water by metal ions (Al^{3+} , La^{3+} and ZrO^{2+}) loaded natural zeolite," *Separation Science and Technology*, vol. 42, no. 9, pp. 2033–2047, 2007.
- [41] C. Díaz-Nava, M. T. Olguín, and M. Solache-Ríos, "Water defluoridation by Mexican heulandite-clinoptilolite," *Separation Science and Technology*, vol. 37, no. 13, pp. 3109–3128, 2002.
- [42] J. Lu, D. Liu, J. Hao, G. Zhang, and B. Lu, "Phosphate removal from aqueous solutions by a nano-structured Fe–Ti bimetal oxide sorbent," *Chemical Engineering Research and Design*, vol. 93, pp. 652–661, 2015.
- [43] F. Ogata, D. Imai, M. Toda, M. Otani, and N. Kawasaki, "Adsorption of phosphate ion in aqueous solutions by calcined cobalt hydroxide at different temperatures," *Journal of Environmental Chemical Engineering*, vol. 3, no. 3, pp. 1570–1577, 2015.
- [44] H. Li, J. Ru, W. Yin, X. Liu, J. Wang, and W. Zhang, "Removal of phosphate from polluted water by lanthanum doped vesuvianite," *Journal of Hazardous Materials*, vol. 168, no. 1, pp. 326–330, 2009.
- [45] J. Xie, Z. Wang, D. Fang, C. Li, and D. Wu, "Green synthesis of a novel hybrid sorbent of zeolite/lanthanum hydroxide and its application in the removal and recovery of phosphate from water," *Journal of Colloid and Interface Science*, vol. 423, pp. 13–19, 2014.
- [46] G. Li, D. Chen, W. Zhao, and X. Zhang, "Efficient adsorption behavior of phosphate on La-modified tourmaline," *Journal of Environmental Chemical Engineering*, vol. 3, no. 1, pp. 515–522, 2015.
- [47] V. Sivasankar, T. Ramachandramoorthy, and A. Chandramohan, "Fluoride removal from water using activated and MnO_2 -coated Tamarind Fruit (*Tamarindus indica*) shell: batch and column studies," *Journal of Hazardous Materials*, vol. 177, no. 1–3, pp. 719–729, 2010.
- [48] S. Deng, H. Liu, W. Zhou, J. Huang, and G. Yu, "Mn-Ce oxide as a high-capacity adsorbent for fluoride removal from water," *Journal of Hazardous Materials*, vol. 186, no. 2-3, pp. 1360–1366, 2011.
- [49] J. Cheng, X. Meng, C. Jing, and J. Hao, " La^{3+} -modified activated alumina for fluoride removal from water," *Journal of Hazardous Materials*, vol. 278, pp. 343–349, 2014.
- [50] Y. Zhang, Y. Xu, H. Cui et al., "La(III)-loaded bentonite/chitosan beads for defluoridation from aqueous solution," *Journal of Rare Earths*, vol. 32, no. 5, pp. 458–466, 2014.
- [51] S. Zhang, Y. Lu, X. Lin, X. Su, and Y. Zhang, "Removal of fluoride from groundwater by adsorption onto La(III)- Al(III) loaded scoria adsorbent," *Applied Surface Science*, vol. 303, pp. 1–5, 2014.
- [52] S.-X. Teng, S.-G. Wang, W.-X. Gong, X.-W. Liu, and B.-Y. Gao, "Removal of fluoride by hydrous manganese oxide-coated alumina: performance and mechanism," *Journal of Hazardous Materials*, vol. 168, no. 2-3, pp. 1004–1011, 2009.
- [53] Y. C. Sharma, Uma, and S. N. Upadhyay, "Removal of a cationic dye from wastewaters by adsorption on activated carbon developed from coconut coir," *Energy and Fuels*, vol. 23, no. 6, pp. 2983–2988, 2009.
- [54] S. K. Swain, S. Mishra, T. Patnaik, R. K. Patel, U. Jha, and R. K. Dey, "Fluoride removal performance of a new hybrid sorbent of Zr(IV)-ethylenediamine," *Chemical Engineering Journal*, vol. 184, pp. 72–81, 2012.
- [55] S. Lagergren, "Zur theorie der Sogenannten adsorption geloster stoffe," *K. Sven. Vetenskapsakad Handl*, vol. 24, pp. 1–39, 1898.

- [56] C. W. Cheung, J. F. Porter, and G. McKay, "Sorption kinetic analysis for the removal of cadmium ions from effluents using bone char," *Water Research*, vol. 35, no. 3, pp. 605–612, 2001.
- [57] I. Langmuir, "The constitution and fundamental properties of solids and liquids," *Journal of the American Chemical Society*, vol. 39, pp. 2221–2295, 1916.
- [58] H. M. F. Freundlich, "Über die adsorption in losungen," *Zeitschrift Fur Physikalische Chemie A*, vol. 57, pp. 385–470, 1906.
- [59] S. Tian, P. Jiang, P. Ning, and Y. Su, "Enhanced adsorption removal of phosphate from water by mixed lanthanum/aluminum pillared montmorillonite," *Chemical Engineering Journal*, vol. 151, no. 1–3, pp. 141–148, 2009.
- [60] K. Biswas, S. K. Saha, and U. C. Ghosh, "Adsorption of fluoride from aqueous solution by a synthetic iron(III)-aluminum(III) mixed oxide," *Industrial and Engineering Chemistry Research*, vol. 46, no. 16, pp. 5346–5356, 2007.
- [61] C.-K. Na and H.-J. Park, "Defluoridation from aqueous solution by lanthanum hydroxide," *Journal of Hazardous Materials*, vol. 183, no. 1–3, pp. 512–520, 2010.
- [62] S. N. Milmlie, J. V. Pande, S. Karmakar, A. Bansiwala, T. Chakrabarti, and R. B. Biniwale, "Equilibrium isotherm and kinetic modeling of the adsorption of nitrates by anion exchange Indion NSSR resin," *Desalination*, vol. 276, no. 1–3, pp. 38–44, 2011.



Hindawi

Submit your manuscripts at
<https://www.hindawi.com>

